Biochemical Pharmacology, Vol. 21, pp. 1–16. Pergamon Press, 1972. Printed in Great Britain

IN VITRO–IN VIVO CORRELATION OF DRUG METABOLISM—DEAMINATION OF 1-β-D-ARABINOFURANOSYLCYTOSINE

R. L. DEDRICK, D. D. FORRESTER and D. H. W. HO*

Biomedical Engineering and Instrumentation Branch, Division of Research Services, National Institutes of Health, Public Health Service, United States Department of Health, Education and Welfare, Bethesda, Md. 20014, U.S.A.

(*Received* 12 *February* 1971; *accepted* 21 *May* 1971)

Abstract—A pharmacokinetic model is presented to permit rational use of enzyme activities and Michaelis constants determined *in vitro*. It is based on physiologic and anatomic principles and is validated by comparison of predicted urinary excretion of 1-β-D-arabinofuranosylcytosine and its metabolite with published data from humans. Model predictions are compared with new data on plasma concentrations of the drug and its metabolite as functions of time after intravenous pulse doses of 1·2 and 86 mg/kg of the parent compound.

IN THE course of our investigation of the pharmacology of 1-β-D-arabinofuranosylcytosine (Ara-C), it became clear that this would be an excellent drug with which to attempt the direct application of metabolic data *in vitro* to predict plasma concentrations observed in man. Ara-C is a cytotoxic agent that has evoked considerable excitement for the treatment of certain neoplasms. It has been observed[1] that intravenously administered Ara-C disappears from the blood of patients more rapidly than can be accounted for by excretion in the urine. It was also shown that Ara-C is deaminated to form 1-β-D-arabinofuranosyluracil (Ara-U) by homogenates of human liver. Camiener and Smith[2] measured the pyrimidine nucleoside deaminase activity of a number of tissues of several mammalian species, including man, and conducted preliminary studies of characterization and inhibition. Ara-U was shown to be a significant inhibitor of Ara-C deamination only when the molar ratio of Ara-U to Ara-C was large. Subsequently Camiener[3,4] studied the deamination reaction in detail with human liver preparations and concluded that the enzyme was present in large amount and was specific in its substrate requirements; no cofactor requirements or direct regulatory mechanism were demonstrated.

As reviewed by Kassel *et al.*,[5] it is thought that Ara-C must be phosphorylated to nucleotide as a requirement for its action. Alternate mechanisms of subsequent biological effect have been proposed. It is now believed that the nucleotide is an inhibitor of DNA polymerase.

The purpose of this report is to show how enzyme kinetics *in vitro* reported by Camiener and Smith[2] can be used in conjunction with a mathematical model of the distribution and excretion of Ara-C and Ara-U to predict plasma concentrations in

* M. D. Anderson Hospital and Tumor Institute, The University of Texas, Houston, Texas 77025.

man after a single intravenous dose of the parent compound. The model is tested for its ability to simulate published information on blood radioactivity and urinary excretion.

Development of model

Development of pharmacokinetic compartmental models on physiological bases has been discussed in a number of contexts.[6–9] We have insisted that all compartments have a real anatomic or physiologic significance and that parameters generally be obtained from or verified by data independent of those which are simulated. Such models are particularly useful for cytotoxic drugs because they permit rational explanation of species differences in drug distribution and offer the possibility of predicting the actual local environment of any target or normal cells as a function of dose schedule and route of administration. The ability to predict local concentrations, in conjunction with information on cell sensitivity, may then provide a reasonable way to optimize therapeutic effect at an acceptable level of toxicity.

Physiological models are essential if enzyme kinetics *in vitro* are to be applied to experiments *in vivo*. With such models, enzymes can be properly localized in the body, saturation effects and flow limitations can be incorporated, and intratissue transport can be included if necessary.

Any model which describes the pharmacokinetics of Ara-C must account for what has been observed regarding its distribution. After an intravenous injection of a small dose of radioactively labeled Ara-C: (1) initially, blood (or plasma) radioactivity decreases very rapidly followed by a slow exponential decrease; (2) the radioactivity is rapidly and almost quantitatively excreted in the urine; and (3) urinary radioactivity is only a small percentage Ara-C, which is primarily excreted within a short time interval.[10,11] Ara-C is very soluble in water and not significantly bound to plasma proteins of dogs.[12] Radioactivity, given as Ara-C, is rapidly distributed between blood and a variety of normal tissues in mice, with a ratio of radioactivity in tissues to that in blood of approximately unity; the brain is an important exception.[13] Neil *et al.*[14] have reported Ara-C and Ara-U concentrations in mouse plasma. After intraperitoneal injection, they obtained a plasma half-life of Ara-C of about 20 min. There was a corresponding increase in the fraction of plasma radioactivity associated with Ara-U, reaching about 60 per cent at 1 hr and 70 per cent at 2 hr. Kessel *et al.*[5] have studied the uptake and phosphorylation of Ara-C by normal and leukemic human blood cells *in vitro*. They observed a very rapid uptake of the drug (even at 10°) and a cell to medium distribution ratio of unity over a wide range of drug concentrations.

Compartmental model. Figure 1 shows a model suggested by existing data. Lumped compartments representing the liver, kidneys and heart are chosen, in part, to enable the use of enzyme activity data *in vitro*. The lean tissue appears to be an important reservoir for drug and metabolite. The marrow has been represented because it is a critical site of toxicity. The gastrointestinal tract is included to enable potential simulation of oral doses or metabolic activity without essential change in the model.

*Model equations.** The mathematical model consists of a set of mass-balance equations on each compartment for Ara-C and Ara-U. These are based on the concept

*The derivation of the mathematical model and a statement of its major assumptions are outlined here. A detailed derivation including a rigorous analysis of the concept of flow limitation is contained in Appendix A.

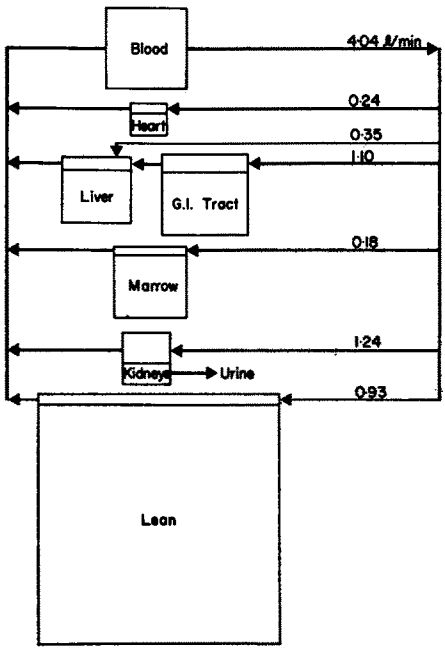

FIG. 1. Compartmental model for Ara-C pharmacokinetics. The compartment volumes are approximately proportional to areas on the figure. Compartment perfusion rates are indicated.

of "flow limitation" in the sense that the drug concentration in the blood leaving any compartment is in equilibrium with the concentration in the tissue. They also incorporate the assumption that the tissue to blood equilibrium distribution ratio is unity for both Ara-C and Ara-U so that venous blood leaving a compartment represents the tissue concentration. This assumption is suggested by the work of Uchida and Kreis[13] considered together with the observations of Neil *et al.*[14] in the mouse; the tissue to blood ratio for total radioactivity remains approximately unity while the plasma radioactivity is converted from essentially 100 per cent Ara-C to 30 per cent Ara-C and 70 per cent Ara-U. Phosphorylation of the drug and subsequent hydrolysis or other metabolic fate of the intracellular nucleotide are not included in the model. Enzyme kinetics are based on compartment concentrations.
For the kidney,

$$V_K \frac{dC_K}{dt} = Q_K C_B - Q_K C_K - k_K C_B - \left(\frac{v_{max,K} C_K}{K_{m,K} + C_K}\right) V_{KT} \qquad (1)$$

Accumulation of drug | Rate of inflow with blood | Rate of outflow with blood | Clearance by kidney | Rate of metabolism

where V = compartment size (ml or g), C = concentration (μg/ml or μg/g), t = time (min), Q = blood flow rate to organ (ml/min), k = clearance (ml/min), v_{max} = enzyme activity at saturation [μg/(g) (min)], K_m = Michaelis constant (μg/ml), and the subscripts K and KT refer to the kidney (including equilibrium blood) and kidney tissue. The metabolism term serves operationally to define v_{max} and K_m *in vivo* based on a uniform compartment. Similar equations, without the clearance term, are written for the heart, gastrointestinal tract, marrow and lean tissue. The balance on the liver

differs only slightly from Equation 1, since blood reaches it from both the arterial and portal circulation. Finally, the balance on the blood compartment is

$$V_B \frac{dC_B}{dt} = (Q_H C_H + Q_{Li} C_{Li} + Q_M C_M + Q_K C_K + Q_{Le} C_{Le}) - Q_B C_B$$

Accumulation of drug — Rate of inflow from tissue compartments — Rate of outflow to tissue compartments

$$- \left[\frac{v_{max,B} C_B}{K_{m,B} + C_B}\right] V_B + Mg(t) \qquad (2)$$

Rate of metabolism — Rate of injection

where M = dose of drug (μg), $g(t)$ = injection function (min^{-1}),[6] and the subscripts have the expected meaning.

The cumulative excretion, U, of drug in the urine is

$$U = \int_0^t k_K C_B \, dt. \qquad (3)$$

A similar set of equations is written for Ara-U. It is identical to the above, except that the terms representing metabolism have a positive sign, since the metabolite is being formed. After selection of suitable parameters, the equations are solved simultaneously using a digital computer. The results include numerical values of predicted concentrations of Ara-C and Ara-U in each of the seven compartments and cumulative urinary excretion as functions of time.

Estimation of parameters. The parameters necessary for the solution of the model equations include organ sizes, blood flow rates, kidney clearance, enzyme activities and Michaelis constants. Since Ara-C and Ara-U, which is derived from the former by simple hydrolytic deamination, are structurally similar, it is assumed that their distribution between plasma and tissue is substantially the same, as discussed above, and that the kidney clearance inferred from total radioactivity can be used for both.

Table 1 contains the parameters that were used in all simulations. The volumes and flows are primarily derived from Mapleson[15] as described in Appendix B. Volumes include both the tissue and the equilibrium blood. The kidney clearance in Table 1 was inferred from the blood radioactivity data of Creasey *et al.*[10] for two adult male patients who received intravenous injections of 5 and 10 mg/kg. These patients showed blood levels proportional to dose at all times. (One woman who received 10 mg/kg exhibited blood levels closer to those of the lower dose in the men.) In order to achieve an adequate simulation of blood radioactivity of the two men, it was necessary to reduce the total volume. Mathematically, this was accomplished by decreasing the volume of the lean compartment from 41 l. as derived in Appendix B to 27 l. as shown in Table 1. This was the only anatomic parameter used which was not derived independently of any data to be simulated. The required decrease probably reflects individual differences that occur between standard parameters and those appropriate to any individual. It may also reflect a minor departure from unity in tissue to blood equilibrium ratios and suggests that an alternate basis for the balances would be the water content of tissues.

TABLE 1. MODEL PARAMETERS FOR STANDARD 70 kg MAN

Compartment	Volume (l.)	Flow (l./min)	Michaelis constant (μg/ml)	Deaminase activity [μg/(g)(min)]	Clearance (ml/min)
Blood	2·67	4·04			
Liver	1·70	1·45	27*	119*	
Gut	3·18	1·10			
Heart	0·448	0·24	(31)†	6‡	
Kidney	1·06	1·24	(32)†	20‡	90
Lean	27·0	0·93			
Marrow	2·00	0·18			

* G. W. Camiener, *Biochem. Pharmac.* **16,** 1981 (1967); Michaelis constant adjusted for water content.

† The Michaelis constants for heart and kidney were estimated equal to that for liver on a water content basis.

‡ G. W. Camiener and C. G. Smith, *Biochem. Pharmac.* **14,** 1405 (1965).

EXPERIMENTAL

Ara-C (NSC-63878), Ara-C-^{3}H and tetrahydrouridine (THU) were supplied by the Drug Development Branch of the Cancer Chemotherapy National Service Center, National Cancer Institute. The radiochemical purity was over 97 per cent. Ara-U was purchased from Calbiochem, Los Angeles, Calif.

Patients with acute myelogenous leukemia and lymphoma, but with normal hepatic and renal functions, were intravenously injected with 1·2–86 mg/kg of Ara-C containing 0·5 mc of generally labeled Ara-C-^{3}H (specific activity, 10·75 mc/m-mole). Heparinized blood samples were collected at indicated intervals with 1×10^{-4} M THU, an inhibitor of the pyrimidine nucleoside deaminase. The samples were immediately immersed in an ice bath and then centrifuged at 4° to separate the cells and plasma. Plasma samples were denatured by the addition of perchloric acid to a final concentration of 5%. The supernatant was neutralized with potassium hydroxide and applied to Whatman No. 1 filter paper. Paper chromatograms were developed in a solvent system (isopropanol–H_2O–ethyl acetate, 13·7:7·3:39) with descending flow. The radioactive spots were identified with authentic compounds by ultraviolet absorption and radioscanning. The spots were cut out, eluted with 1 ml water, and counted with 10 ml of 10% BBS (Beckman Bio-Solv) counting solution. The counting efficiency for tritium was approximately 35 per cent. The R_f values for Ara-C and Ara-U were 0·1 and 0·32 respectively. The addition of THU did not change the R_f values. Heparin did not interfere with the extractability of Ara-C or Ara-U from blood or with the R_f values for Ara-C or Ara-U.

RESULTS AND DISCUSSION

Comparison with published data

The major features of the model predictions are illustrated in Fig. 2 for an i.v. dose of 10 mg/kg injected in 1 min. In Fig. 2 and subsequently, weight concentrations are expressed on the basis of the hydrochloride salt. Figure 2 shows a very rapid fall in the blood Ara-C concentration resulting from both redistribution into tissues and metabolism in the liver, heart and kidney. After about 10 min, the lean compartment

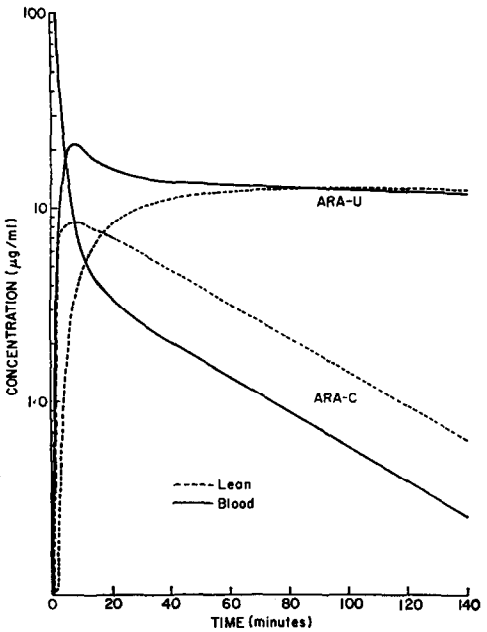

FIG. 2. Model predictions of the concentration of Ara-C and Ara-U in the blood and lean compartments after a pulse dose of 10 mg/kg in a 70 kg man.

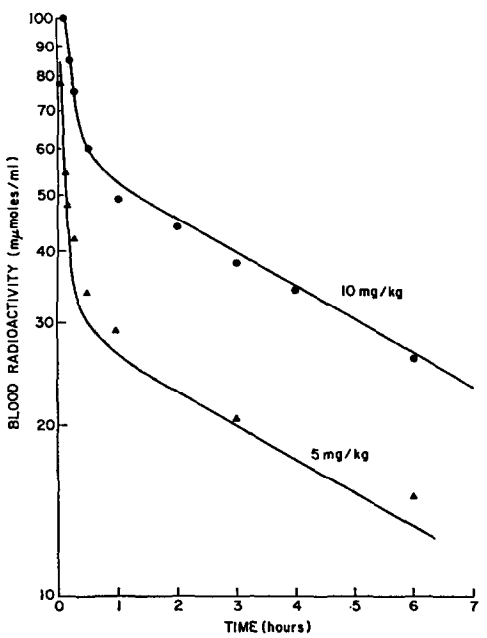

FIG. 3. Model simulations of blood radioactivity (solid lines) compared with experimental data of Creasey *et al.*[10] for i.v. administration in two men.

serves as a reservoir of parent drug so that the blood Ara-C concentration is maintained at a lower rate of decrease. With the parameters selected, the Ara-U does not approach perfusion equilibrium for about an hour.

Figure 3 illustrates the ability of the model to simulate blood radioactivity (Ara-C plus Ara-U) data from the literature.[10] This is not a total model validation because the lean tissue volume was adjusted for these two sets of data, as discussed previously, and the kidney clearance was inferred from these data also. The kidney clearance of 90 ml/min, which simulates the data of Creasey *et al.*[10] in the context of the model compares with a published plasma clearance of 147 ml/min (corrected to 1·73 m^2) for a 15-year-old child.[11]

An independent measure of kidney clearance is obtained from the prediction of cumulative urinary radioactivity as shown in Fig. 4, where published data are compared with the model prediction for periods up to 8 hr. Figure 5 presents the predicted split between Ara-C and Ara-U in the urine and compares these with published data.

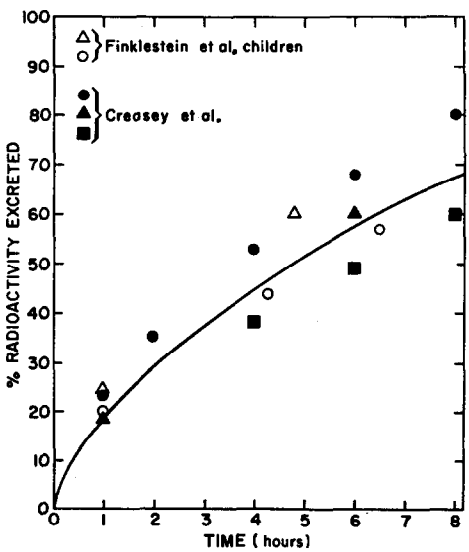

FIG. 4. Model predictions (solid line) vs. published data for cumulative urinary excretion of radioactivity after i.v. administration.

Seven and one-half per cent of the dose is predicted as Ara-C; Creasey *et al.*[10] reported 6·5 to 10 per cent. At higher doses, enzyme saturation effects would be expected to result in a larger fraction of Ara-C in the urine.

Prediction of plasma concentration of Ara-C

Figures 3–5 have been presented to verify the ability of the model to simulate Ara-C and Ara-U distribution and excretion. Since the purpose of this work is to demonstrate direct application of enzyme kinetic data *in vitro* to predictions in the situation *in vivo*, simulations of plasma concentration of Ara-C after i.v. injections of 1·2 and 86 mg/kg were conducted. These predictions are compared with experimental data in Figs. 6 and 7. The two dose levels were chosen to cover a wide range (72:1) and because

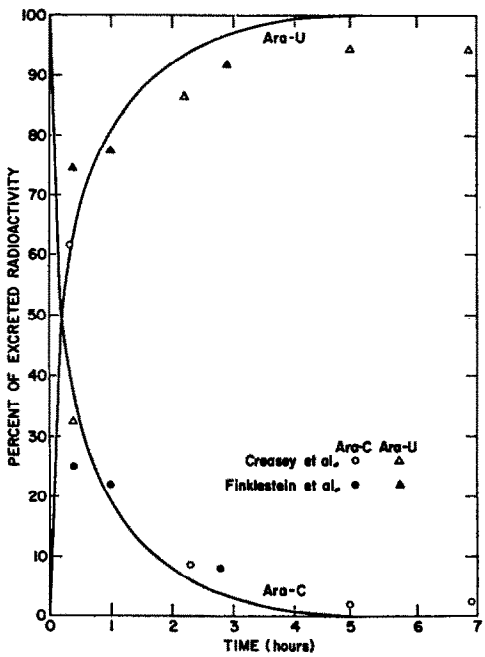

FIG. 5. Model prediction of split between Ara-C and Ara-U in the urine. The model curves are predicted for an i.v. pulse of 10 mg/kg. The data represent i.v. administration of 5 mg/kg, 10 mg/kg or 24–219 mg/m² (ca. 1–9 mg/kg).

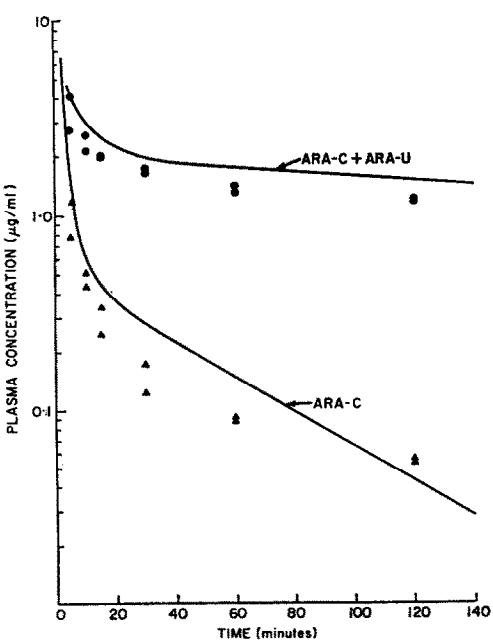

FIG. 6. Predicted concentrations of Ara-C and total radioactivity in the plasma after a pulse dose of 1·2 mg/kg, i.v. Data points represent two different injections of Ara-C in a 70 kg woman.

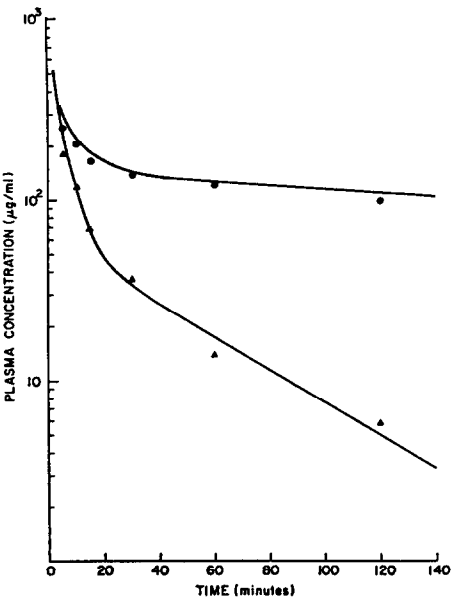

FIG. 7. Predicted concentrations of Ara-C and total radioactivity in the plasma after a pulse dose of 86 mg/kg, i.v. Data points represent measured concentrations in the plasma of a 52 kg woman.

simulations of total radioactivity were sufficiently successful in these patients that a valid estimate of the effect of metabolism could be made. Individual variations in body water and other relevant factors are quite large; one cannot expect to predict actual concentrations in body regions more precisely than these region sizes, related flows and other physiologic parameters are known. Critical parameters can be estimated for an individual if a high degree of predictive accuracy is required. The usefulness of such models in accounting for species differences and enhancing pharmacologic insight is clear.

Figures 6 and 7 show quite close agreement between the predicted and observed plasma concentration of Ara-C, even though its concentration is reduced by metabolism to a small fraction of total radioactivity in a very short time. The data are about 35 per cent lower than the estimate during the period from 15 to 60 min at the lower dose. This discrepancy is not surprising in view of the reported variation in liver deaminase activity of 66–168 (mean 119) μg/(g)(min).[2] Also, metabolism by all tissues other than liver, kidney and heart has been neglected, and small rates of metabolism by these other tissues could be a source of discrepancy. Another factor affecting the rate of metabolism is the perfusion rates of the various metabolically active and inactive compartments. The model underpredicts plasma Ara-C concentration seriously at long times (not shown). This suggests that one or more additional "deep" compartments (e.g. bone cortex, brain, skin) may be required to complete the overall pharmacokinetic picture. In addition, the possible importance of slow hydrolysis of intracellular Ara-C-nucleotide in releasing Ara-C has not been assessed.

We have not attempted a detailed analysis of the sensitivity of the model to parameter changes. The rationale in presenting Figs. 6 and 7 is to show a comparison

between data and a totally *a priori* estimate of expected plasma concentrations consistent with the model assumptions. Figure 8 shows the results obtained when a lean tissue volume of 41 l. (derived in Appendix B) and a hepatic perfusion rate of 2·0 l./min are used. All other parameters, including the Michaelis constant and deaminase activities, are the same as reported in Table 1. The changes in lean tissue volume and hepatic perfusion rate are well within physiologic limits and result in a substantially improved "fit" to the experimental data. This illustrates how metabolism *in vivo* can be affected by purely anatomic or physiologic variables without any change in the local enzyme amount or kinetics.

Both the model and the limited experimental data indicate that plasma concentrations of Ara-C increase more rapidly than the dose over the dose range studied. This suggests the possibility of saturation effects of the enzyme system. Such effects are also suggested by comparing the observed plasma concentration with the Michaelis constant of 27 μg/ml (based on whole tissue of liver). The deamination by any metabolically active tissue is assumed to be of the form (e.g. Equations 1 and 2) $\left(\frac{v_{max}C}{K_m + C}\right)V$. Clearly, at the low dose of 1·2 mg/kg (Fig. 6), the plasma concentration and the tissue concentrations are much less than the Michaelis constant at essentially all times. This means that the metabolism terms take the form $\left(\frac{v_{max}C}{K_m}\right)V$, and the rate of deamination is simply proportional to the drug concentration in the tissue, C. At the high dose of 86 mg/kg (Fig. 7), short-time plasma concentrations greatly exceed the Michaelis constant so that the *relative* rate of deamination can be less.

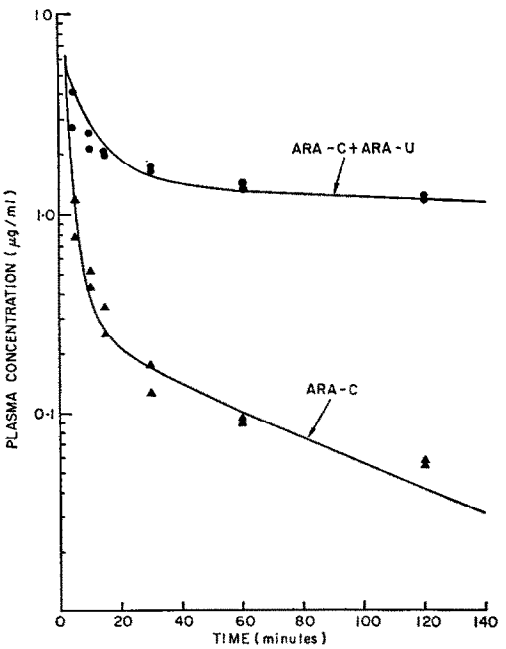

FIG. 8. Model simulations of Ara-C and total radioactivity in the plasma after a pulse dose of 1·2 mg/kg, i.v. Data points represent two different injections of Ara-C in a 70 kg woman (see Fig. 6). Solid lines are model simulations with parameters adjusted as discussed in text.

While the ability to predict plasma concentrations, at least semiquantitatively, has been demonstrated, it is not felt that the work presented here provides a complete test of the *local* kinetics of Ara-C metabolism *in vivo*. It appears that about 80 per cent of the drug that reaches the liver may be metabolized at low blood concentrations. If flow limitation of the drug is approached this closely, a relatively imprecise estimate of enzyme kinetics in the liver or gastrointestinal tract would not exert a profound effect on expected systemic results. Metabolism by any of the peritoneal organs whose venous outflow is channeled through the liver would tend to be obscured, since the model and observed plasma concentrations would not be particularly sensitive to such metabolism.

A large number of assumptions have been made in order to develop the full set of model equations as shown in Appendix A, and very many physiologic, anatomic and biochemical parameters are required. Most of these are known within reasonable limits; however, one should use extreme caution in generalizing from the model. It must currently be considered preliminary. Inability, at present, to incorporate the clinically important phosphorylation seriously limits its applicability to predict cytotoxicity. Metabolism by other compartments can be included as more data are acquired, and the assumption that the same Michaelis constant determined *in vitro* is representative of all local metabolism *in vivo* can be relaxed. A rather serious problem may occur for any drug such as this, which is metabolized so rapidly that very large intertissue concentration differences occur, because venous blood sampled may not represent well the average concentration in the blood compartment. This may be a special problem if blood is drawn from a small peripheral vein draining a very poorly perfused region without significant shunt flow. Further, and also of possible significance, the assumption of flow limitation has not been documented rigorously in all tissue.

Very few data are available on the detailed distribution of Ara-U. There is strong suggestive evidence that its transport and equilibrium distribution ratio between tissue and plasma are rather similar to those of Ara-C, as discussed previously. The assumed kidney clearance can be validated rigorously by comparing measured plasma concentrations with the cumulative mass of metabolite in the urine as suggested by Equation A19 (Appendix A) written for Ara-U.

The postulate of a large and slowly or nonmetabolizing compartment, assigned here to the muscle and skin, has not been confirmed experimentally by direct measurement. Further, metabolism by all tissues other than heart, kidney and liver has been neglected, and large activity in a well perfused region or quite small activity in a large poorly perfused region could have some contribution.

In summary, the enzyme system chosen required a rather complex model of the overall pharmacokinetics of the drug and its metabolite to permit rational use of data *in vitro* to predict metabolism *in vivo*. Within the context of the pharmacokinetics, enzyme activities and Michaelis constants have been used directly in the appropriate organ volumes. This provides total organ activities and permits description of *local* saturation effects and flow limitations which would be impossible to describe if a nonphysiologic model were used.

Acknowledgements—The authors wish to acknowledge helpful discussions with Dr. Gary L. Neil during the initial phases of this work. An intellectual debt is owed Dr. Kenneth B. Bischoff for his pioneering thinking in pharmacologic modeling.

REFERENCES

1. R. V. LOO, M. J. BRENNAN and R. W. TALLEY, *Proc. Am. Ass. Cancer Res.* **6**, 41 (1965).
2. G. W. CAMIENER and C. G. SMITH, *Biochem. Pharmac.* **14**, 1405 (1965).
3. G. W. CAMIENER, *Biochem. Pharmac.* **16**, 1681 (1967).
4. G. W. CAMIENER, *Biochem. Pharmac.* **16**, 1691 (1967).
5. D. KESSEL, T. C. HALL and D. ROSENTHAL, *Cancer Res.* **29**, 459 (1969).
6. K. B. BISCHOFF and R. L. DEDRICK, *J. pharm. Sci.* **57**, 1346 (1968).
7. R. L. DEDRICK and K. B. BISCHOFF, *Chem. Engng Prog. Symp. Ser. 84*, **64**, 32 (1968).
8. K. B. BISCHOFF, R. L. DEDRICK and D. S. ZAHARKO, *J. pharm. Sci.* **59**, 149 (1970).
9. H. L. GABELNICK, R. L. DEDRICK and R. S. BOURKE, *J. appl. Physiol.* **28**, 636 (1970).
10. W. A. CREASEY, R. J. PAPAC, M. E. MARKIW, P. CALABRESI and A. D. WELCH, *Biochem. Pharmac.* **15**, 1417 (1966).
11. J. Z. FINKLESTEIN, J. SCHER and M. KARON, *Cancer Chemother. Rep.* **54**, 35 (1970).
12. R. L. DIXON and R. H. ADAMSON, *Cancer Chemother. Rep.* **48**, 11 (1965).
13. K. UCHIDA and W. KREIS, *Biochem. Pharmac.* **18**, 1115 (1969).
14. G. L. NEIL, T. E. MOXLEY and R. C. MANAK, *Cancer Res.* **30**, 2166 (1970).
15. W. W. MAPLESON, *J. appl. Physiol.* **18**, 197 (1963).
16. D. KESSEL and S. B. SHURIN, *Biochim. biophys. Acta* **163**, 179 (1968).
17. J. A. LARSEN, *Nature, Lond.* **184**, 1236 (1959).
18. F. PITTS, *Physiology of the Kidney and Body Fluids.* Year Book Medical Publishers, Chicago (1963).
19. K. B. BISCHOFF and R. G. BROWN, *Chem. Engng Prog. Symp. Ser. 66*, **12**, 33 (1966).
20. A. C. GUYTON, *Textbook of Medical Physiology*, 5th edn. Saunders, Philadelphia (1968).
21. R. M. FORBES, A. R. COOPER and H. H. MITCHELL, *J. biol. Chem.* **203**, 361 (1953).

APPENDIX A

Derivation of model equations. The construction of the model equations is based on the concept of a compartment. In this context, a compartment is an organ, a tissue or some combination of tissues which may be grouped for purposes of analysis. This grouping requires that the tissues which comprise a compartment be similar in those parameters relevant to drug distribution. These include the perfusion rate [expressed as a volume of blood per unit time per unit tissue volume, e.g. (milliliters of blood per minute or per milliliter or gram of tissue)]; physicochemical properties such as the parameters necessary to describe lipid solubility or protein binding; operational metabolic constants in the compartment; and appropriate measures of physiologic function such as kidney clearance, biliary excretion and intestinal or other absorption.

Figure 9 shows a typical compartment. If metabolism occurs in the compartment, it would normally be confined to the tissue and be a function of the drug concentration there.

In the general case, the drug may be free, with its concentration equal to C, or bound, e.g. to plasma or tissue proteins, with a concentration x. Thermodynamically, the bound concentration is a function of the free concentration through relationships which may be determined empirically:

$$x_{TB} = f(C_{TB}) \tag{A1}$$

$$x_T = F(C_T). \tag{A2}$$

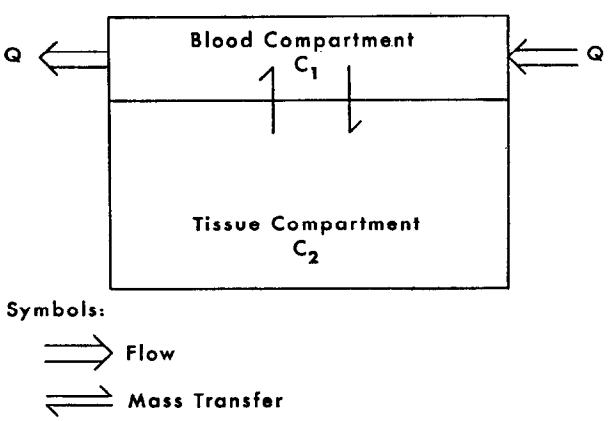

FIG. 9. Typical body compartment showing tissue and blood.

If the drug is not significantly bound to plasma proteins, mass-balance equations on the two parts of the compartment take the form

$$V_1 \frac{dC_1}{dt} = Q(C_0 - C_1) + p\left(\frac{C_2}{K} - C_1\right) \tag{A3}$$

$$V_2 \frac{dC_2}{dt} = p\left(C_1 - \frac{C_2}{K}\right) \tag{A4}$$

where K represents the equilibrium distribution ratio between blood and tissue, p is the permeability, and C_0 is the concentration of the drug in the blood entering the compartment. Equations A3 and A4 and their detailed analysis, which follows, are from reference 7.
For the case if flow-limiting conditions, $p \to \infty$, Equations A3 and A4 become

$$(V_1 + KV_2)\frac{dC_1}{dt} = Q(C_0 - C_1). \tag{A5}$$

The solution of equation A5 for a pulse injection of M units of drug is

$$(C_1)_\infty = \frac{M}{Q}\left(\frac{Q}{V_1 + KV_2}\right) e^{-[Q/(V_1+KV_2)]t}. \tag{A6}$$

This may be compared with the general solution of Equations A3 and A4 for a finite membrane permeability.

$$C_1 = \frac{M}{Q}\frac{Q}{V_1}\frac{\left(r_2 + \frac{p}{KV_2}\right)e^{r_2 t} - \left(r_1 + \frac{p}{KV_2}\right)e^{r_1 t}}{2R} \tag{A7a}$$

where

$$r_{(\frac{1}{2})} = -\frac{1}{2}\left[\frac{Q}{V_1} + \frac{p}{V_1}\left(1 + \frac{V_1}{KV_2}\right)\right] \mp R \tag{A7b}$$

$$R = \sqrt{\left(\frac{1}{4}\left[\frac{Q}{V_1} + \frac{p}{V_1}\left(1 + \frac{V_1}{KV_2}\right)\right]^2 - \frac{Qp}{V_1 KV_2}\right)}. \tag{A7c}$$

Now, in the limit as $p \to \infty$, the root r_1 becomes very large and negative, and Equation A7a reduces to equation A6.

In order to derive a mathematical criterion for flow-limiting conditions, a formal expansion of Equation A7 in terms of (Q/p) can be made, and the result is

$$C_1 = \frac{M}{Q}\left(\frac{Q}{V_1 + KV_2}\right)\left[1 - \left(\frac{Q}{p}\right)\left(1 + \frac{V_1}{KV_2}\right)^{-2}\right]$$

$$\times \exp\left\{-\left(\frac{Q}{V_1 + KV_2}\right)\left[1 - \left(\frac{Q}{p}\right)\left(1 + \frac{V_1}{KV_2}\right)^{-2}\right]t\right\}$$

$$+ \text{higher order terms in } \frac{Q}{p}. \tag{A8}$$

It is seen that Equation A8 reduces to the flow-limiting case, Equation A6, if the following criterion is satisfied:

$$\frac{Q}{p} \ll \left(1 + \frac{V_1}{KV_2}\right)^2. \tag{A9}$$

For most practical cases, $V_1 \ll KV_2$; so, the right-hand side of Equation A9 is approximately unity. The analysis thus yields the extremely simple criterion for flow-limiting conditions

$$\frac{Q}{p} \ll 1. \tag{A10}$$

The form of Equation A10 is what one would expect intuitively; that is, if the regional perfusion is much smaller than the regional permeability, one can assume that mass transfer by diffusion is relatively very rapid and the only important resistance to mass transport is the flow limitation. A discussion of the experiments conducted to obtain transport parameters *in vivo* is presented in reference 7. These are generally of the constant infusion type.

In applying the concepts developed above to Ara-C, it may be observed that Kessel *et al.*[5] measured a very rapid uptake of the drug even at 10° and a cell to medium distribution ratio of unity over a wide range of drug concentrations. Uchida and Kreis[13] showed that there was no lag between a variety of tissues and blood in the mouse on the time scale of their experiments. In a subline of L1210 leukemia unable to metabolize Ara-C, Kessel and Shurin[16] obtained a cell to medium distribution ratio of unity within 1 min, except at the highest (25 mM) concentration. The liver, which has the highest metabolic activity of the tissues studied in man, is perfused at a rate of about 85 per cent per min, so that the nominal residence time of the drug in the compartment is more than the minute required to achieve equilibrium, at least in the L1210 cells, and a more rapid transport would be expected in the liver. Additional evidence is found in the ability of the liver to clear essentially all of the ethanol reaching it at very low ethanol concentrations in the blood.[17] This shows that for this highly water-soluble drug there are no functional shunts in the sense of alcohol not being exposed intimately to metabolically active tissue.

The evidence thus very strongly suggests that Ara-C approaches flow limitation in its distribution and that the tissue to blood or plasma distribution ratio is essentially unity. Further, it has been demonstrated not to be significantly bound to plasma proteins.[12] With these assumptions, Equation A5 takes the form

$$(V_1 + V_2)\frac{dC}{dt} = Q(C_0 - C) \tag{A11}$$

since $$K = 1.$$

The general Equation A11 may be applied to each of the seven compartments shown in the flow chart of the model (Fig. 1). The possibility of metabolism by a Michaelis–Menten process is included in each compartment, even though there may actually be negligible activity in certain tissues. Removal by the kidney without metabolism can also occur, and the clearance is defined in the usual way.

The complete set of equations for Ara-C is therefore:

Blood:

$$V_B\frac{dC_B}{dt} = (Q_H C_H + Q_{Li} C_{Li} + Q_M C_M + Q_K C_K + Q_{Le} C_{Le}) \tag{A12}$$

Accumulation of drug — Rate of inflow from tissue compartments

$$- Q_B C_B - \left(\frac{v_{max,B} C_B}{K_{m,B} + C_B}\right) V_B + Mg(t)$$

Rate of outflow to tissue compartments — Rate of metabolism — Rate of injection

The terms have been defined earlier. The injection function, $g(t)$, has the form [6]

$$g(t) = 30\,\lambda(\lambda t)^2\,(1 - \lambda t)^2$$

where λ is the reciprocal injection duration, min^{-1}.

Heart:

$$V_H\frac{dC_H}{dt} = Q_H C_B - Q_H C_H - \left(\frac{v_{max,H} C_H}{K_{m,H} + C_H}\right) V_{HT}. \tag{A13}$$

Here, and in the following equations, only the tissue volume is used as a basis for metabolism by the enzyme located in the tissue.

Liver:

$$V_{Li}\frac{dC_{Li}}{dt} = (Q_{Li} - Q_G) C_B + Q_G C_G - Q_{Li} C_{Li} - \left(\frac{v_{max,Li} C_{Li}}{K_{m,Li} + C_{Li}}\right) V_{LiT}. \tag{A14}$$

Gastrointestinal tract:

$$V_G \frac{dC_G}{dt} = Q_G C_B - Q_G C_G - \left(\frac{v_{max,G} C_G}{K_{m,G} + C_G}\right) V_{GT}. \quad \text{(A15)}$$

Marrow:

$$V_M \frac{dC_M}{dt} = Q_M C_B - Q_M C_M - \left(\frac{v_{max,M} C_M}{K_{m,M} + C_M}\right) V_{MT}. \quad \text{(A16)}$$

Kidneys:

$$V_K \frac{dC_K}{dt} = Q_K C_B - Q_K C_K - k_K C_B - \left(\frac{v_{max,K} C_K}{K_{m,K} + C_K}\right) V_{KT}. \quad \text{(A17)}$$

Lean tissue:

$$V_{Le} \frac{dC_{Le}}{dt} = Q_{Le} C_B - Q_{Le} C_{Le} - \left(\frac{v_{max,Le} C_{Le}}{K_{m,Le} + C_{Le}}\right) V_{LeT}. \quad \text{(A18)}$$

Cumulative excretion in urine:

$$U = \int_0^t k_K C_B \, dt. \quad \text{(A19)}$$

In a similar way, equations are written for the metabolite, Ara-U. These are identical to equations A12 through A19, except that the metabolism terms are positive, since the Ara-U is being formed from Ara-C by deamination.

The full set of 16 equations (Equations A12–A19 plus similar equations for the metabolite) is solved routinely on a digital computer without further simplification after suitable parameters are selected. The solutions consist of predicted concentrations of Ara-C and Ara-U in each of the seven compartments and the cumulative urinary excretion of both. It is then straightforward to calculate the ratio of Ara-C to Ara-U in the urine on a cumulative basis or for any time interval.

APPENDIX B

*Model parameter derivation for 70 kg man**

Blood compartment:

Volume = 1·4 (Arterial blood)[15] + 0·795 (skin shunt venous blood)[15]
+ 0·371 (equilibrium blood gray matter)[15]
+ 0·100 (equilibrium blood white matter)[15]
= 2·67 l.

Liver compartment:

Volume of tissue = 1·610 l[18]
Volume of equilibrium blood = 0·086 l.[19]
Total volume of compartment = 1·70 l.
Flow = 1·45 l./min.[20]

Gut compartment:

Volume of tissue = 3·90[15] − 1·61[18] = 2·29 l.
Volume of equilibrium blood = 0·976[15] − 0·086[19] = 0·890 l.
Total volume of compartment = 3·18 l.
Flow = 1·10 l./min.[20]

Kidney compartment:

Volume of tissue = 0·300 l.[15]
Volume of equilibrium blood = 0·765 l.[15]
Total volume of compartment = 7·06 l.
Flow = 1·24 l./min.[15]

*The superscript numbers, [15,18–21], are reference numbers.

Heart compartment:

Volume of tissue = 0·300 l.[15]
Volume of equilibrium blood = 0·148 l.[15]
Total volume of compartment = 0·448 l.
Flow = 0·24 l./min.[15]

Lean compartment:

Volume of tissue = 30·0 (muscle)[15] + 3·0 (skin nutritive)[15]
+ 4·8 (non-fat subcutaneous)[15]
+ 11·4 × 0·23 (adipose, corrected to water content)[21]
= 40·4 l.
Volume of equilibrium blood = 0·370 (muscle)[15] + 0·037 (skin nutritive)[15]
+ 0·043 (non-fat subcutaneous)[15] + 0·123 (adipose)[15]
= 0·573 l.
Total volume of compartment = 41·0 l.
Flow = 0·600 (muscle)[15] + 0·060 (skin nutritive)[15]
+ 0·070 (non-fat subcutaneous)[15] + 0·200 (adipose)[15]
= 0·93 l./min.

Marrow compartment:

Volume of tissue = 1·4 (red marrow)[15] + 2·20 (fatty marrow)[15] × 0·23[21]
= 1·90 l.
Volume of equilibrium blood = 0·074 (red marrow)[15] + 0·037 (fatty marrow)[15]
= 0·101 l.
Total volume of compartment = 2·00 l.
Flow = 0·120 (red marrow)[15] + 0·060 (fatty marrow)[15]
= 0·18 l./min.